Quasi-deterministic Proxy for Network-constrained Stochastic Unit Commitment

Xuan Liu, *Member*, *IEEE*, and Antonio J. Conejo, *Fellow*, *IEEE*

***Abstract*—We propose a quasi-deterministic proxy for the network-constrained stochastic unit commitment (SUC) problem. The proposed proxy can identify very similar commitment decisions as those obtained by solving the SUC problem with a large scenario set. Its computational performance, though, is close to that of a deterministic unit commitment problem. The proposed proxy has the same formulation as the SUC problem but only includes one or two envelope scenarios, generated based on the original scenario set. The two envelope scenarios capture the maximum and minimum net-load conditions in the original scenario set. We use a systematic method to assess the quality of commitment decisions obtained by the proposed proxy. The considered case study is based on the Illinois 200-bus system.**

***Index Terms*—Deterministic proxy, network-constrained unit commitment, mixed-integer linear programming, stochastic programming, uncertainty.**

NOMENCLATURE

A. Indices and Sets

Λ_n^{T}	Set of thermal generating units located at bus n
Λ_n^{W}	Set of weather-dependent generating units located at bus n
Λ_n^{N}	Set of nuclear generating units located at bus n
Λ_n^{B}	Set of buses connected to bus n
Ξ	Set of decision variables, $\Xi=\Xi^{\text{1stage}}\bigcup\Xi^{\text{2stage}}$, $\Xi^{\text{1stage}}=\left\{v_{jt},y_{jt},z_{jt}\right\}$, $\Xi^{\text{2stage}}=\left\{p_{jt\omega},p_{it\omega}^{\mathrm{WS}},d_{nt\omega}^{\mathrm{LS}},\theta_{nt\omega}\right\}$
Ψ_j	Feasibility set regarding minimum-up-time and minimum-down-time constraints of generating unit j
ω	Index for scenarios in set Ω
i	Index for weather-dependent generating units in set I
j	Index for thermal generating units in set J
l	Index for nuclear generating units in set L
n,m	Indices for buses
t	Index for time periods in set $T=\left\{1,2,\ldots,\lvert T\rvert\right\}$

B. Parameters

π_ω	Probability of occurrence of scenario ω
B_{nm}	Susceptance of transmission line connecting buses n and m (S)
c^{LS}	Load-shedding cost ($/MWh)
c_i^{W}	Variable cost of weather-dependent generating unit i ($/MWh)
$c_j^{\mathrm{U}},c_j^{\mathrm{D}}$	Start-up and shut-down costs of unit j ($)
c_j^{NL}	No-load cost of unit j ($)
c_j^{V}	Variable cost of unit j ($/MWh)
$D_{nt\omega}$	Power demand at bus n in hour t in scenario ω MW)
n^{Ref}	Index number of reference bus
$\overline{P}_{nm}^{\mathrm{L}}$	Transmission capacity of line connecting buses n and m (MW)
$\overline{P}_j,\underline{P}_j$	The maximum and minimum power outputs of unit j (MW)
$p_{it\omega}^{\mathrm{W}}$	Power output of weather-dependent unit i in hour t in scenario ω (MW)
p_j^{ini}	Power output of unit j at initial time of planning horizon (MW)
p_{lt}^{N}	Power output of nuclear unit l in hour t (MW)
$R_j^{\mathrm{U}},R_j^{\mathrm{D}}$	The maximum ramp-up and ramp-down rates of unit j (MW/h)
$S_j^{\mathrm{U}},S_j^{\mathrm{D}}$	The maximum start-up and shut-down rates of unit j (MW)
v_j^{ini}	Commitment status of unit j at initial time of planning horizon, equal to 1 if online, and 0 otherwise

C. Variables

$\theta_{nt\omega}$	Voltage angle of bus n in hour t in scenario ω (rad)
$d_{nt\omega}^{\mathrm{LS}}$	Load shedding at bus n in hour t in scenario ω (MW)

Manuscript received: September 20, 2024; revised: December 5, 2024; accepted: January 14, 2025. Date of CrossCheck: January 14, 2025. Date of online publication: February 21, 2025.

This work was supported in part by the Advanced Research Projects Agency-Energy (ARPA-E) of U.S. Department of Energy (No. 2171-1618).

X. Liu (corresponding author) is with State Grid Economic Technology Research Institute, Beijing, China (e-mail: liuxuan@chinasperi.sgcc.com.cn).

A. J. Conejo is with the Department of Integrated Systems Engineering and the Department of Electrical and Computer Engineering, The Ohio State University, Columbus, OH 43210, USA (e-mail: conejo.1@osu.edu).

DOI: 10.35833/MPCE.2024.001046

$p_{it\omega}^{\mathrm{WS}}$ Power spillage of weather-dependent generating unit i in hour t in scenario ω (MW)

$p_{jt\omega}$ Power produced by unit j in hour t in scenario ω (MW)

v_{jt} Commitment status of unit j in hour t, equal to 1 if on, and 0 otherwise

y_{jt} Start-up status of unit j in hour t, equal to 1 if it starts up at beginning of hour t, and 0 otherwise

z_{jt} Shut-down status of unit j in hour t, equal to 1 if it shuts down at beginning of hour t, and 0 otherwise

I. Introduction

IN current practice, the power system operator solves a deterministic unit commitment (UC) problem to schedule units by inputting a point forecast of net-load. However, the unit scheduling obtained from such an approach can be either too conservative or insecure [1]. To address this issue and making more effective commitment decisions (in terms of cost and security), a stochastic unit commitment (SUC) problem can be used [2]. The SUC problem characterizes uncertainties via scenarios [3]. We note that a sufficiently large scenario set is required to obtain quality commitment decisions that ensure system security while being economically efficient [4], [5]. However, computational burden (an eventual intractability) is the bottleneck of using the SUC problem in practice.

To drastically reduce the computational burden of a SUC problem while obtaining high-quality commitment decisions, we propose an effective quasi-deterministic UC proxy. The proposed proxy obtains very similar commitment decisions as those from the SUC problem, while its computational burden is close to that of a deterministic UC problem.

Methods to reduce the computational burden of the SUC problem include decomposition, scenario reduction, and relaxation of integer variables.

A parallel Lagrangian relaxation method is proposed in [6] to solve the network-constrained SUC problem. Reference [7] compares the unit-based and scenario-based decomposition methods. A hybrid decomposition method based on the Benders framework is proposed in [8]. Reference [9] develops a stochastic dual dynamic integer programming based decomposition algorithm to solve the multi-stage SUC problem. An adaptive robust optimization model is proposed in [10] to obtain commitment decisions that satisfies the worst scenario. Reference [11] proposes two parallelization and decomposition schemes to speed up a hybrid UC problem that combines both stochastic and robust optimization features.

Regarding scenario reduction, [12] proposes a scenario mapping method to add sufficient ramping information into a reduced scenario set. Reference [13] proposes a scenario reduction method to eliminate low probability scenarios and bundle similar scenarios. Reference [14] uses a sample average approximation method to speed up the solution procedure. References [15], [16] provide comparisons of different scenario reduction methods.

Data-driven relaxation of integer variables is used in [8] and [17]. Reference [18] uses a heuristic genetic algorithm to solve the SUC problem. Such a method generally requires an additional repairing step to ensure the feasibility of commitment decisions regarding physical constraints.

Additionally, [19] proposes to add probabilistic reserve constraints into the deterministic UC problem [19]. Reference [20] proposes a frequency-constrained SUC problem. To reduce its computational burden, they linearize frequency nadir constraints.

Interval optimization for the SUC problem is used in [21]. However, an iterative procedure is required to find upper and lower bounds of the optimal solutions [22]. Reference [23] proposes a hybrid model that combines stochastic programming and interval optimization to improve solution accuracy of commitment decisions while reducing the computational burden.

In recent years, data-driven (learning) methods have been proposed to address the computational challenge of SUC problems [24], [25] and network-constrained UC problems [26]-[29]. These methods speed up the solution procedure by partially fixing binary variables and eliminating redundant inequality constraints in the original problem using different criteria. Such methods are effective but require extensive training or iterative solution processes. Moreover, [30] provides a statistical method to reduce the number of stochastic variables in the SUC problem to ease its computational burden.

The objective of an SUC problem is obtaining optimal commitment decisions. Focusing on this, we note that the extreme scenarios are key to the SUC solution. Considering the literature review above, the contributions of this paper are:

1) To propose a quasi-deterministic proxy for the network-constrained SUC problem. Such proxy can identify very similar commitment decisions as those obtained from solving the stochastic UC problem, being its computational performance is close to that of a deterministic UC problem.

2) To obtain two envelope scenarios from the original scenario set through a simple and interpretable approach. The generated envelope scenarios are composed of data from the original scenario set. Such scenarios include critical information that allows the SUC problem to make effective commitment decisions.

3) To experimentally verify that the commitment decisions obtained using the proposed proxy are generally feasible for all scenarios.

4) To use out-of-sample techniques to characterize the quality of the commitment decision obtained from the proposed proxy.

The remainder of this paper is organized as follows. Section II provides the formulation of the network-constrained SUC model considered in this paper. Section III describes the envelope (extreme) scenarios and the quality metrics considered. Section IV illustrates the main features of proposed proxy using a simple example. Section V provides simulation outcomes using the Illinois 200-bus system. Section VI draws some conclusions.

II. Formulation of Network-constrained SUC Model

The SUC model using a DC power flow description is described in (1), which minimizing the objective function (1a) subject to the first-stage logical conditions (1b)-(1e) and the second-stage operating conditions (per scenario) (1f)-(1n).

$$\min_{\Xi} \sum_t \Bigg\{ \sum_j \left(c_j^{\mathrm{NL}} v_{jt} + c_j^{\mathrm{U}} y_{jt} + c_j^{\mathrm{D}} z_{jt} \right) + \sum_{\omega} \pi_{\omega} \Bigg[\sum_j c_j^{\mathrm{V}} p_{jt\omega} + \sum_i c_i^{\mathrm{W}} \left(p_{it\omega}^{\mathrm{W}} - p_{it\omega}^{\mathrm{WS}} \right) \Bigg] + \sum_{\omega} \sum_n c^{\mathrm{LS}} d_{nt\omega}^{\mathrm{LS}} \Bigg\} \tag{1a}$$

s.t.

$$v_{j,t-1} - v_{jt} + y_{jt} - z_{jt} = 0 \quad \forall j, \forall t \tag{1b}$$

$$v_{j,0} = v_j^{\mathrm{ini}} \quad \forall j \tag{1c}$$

$$\left\{ v_{jt}, y_{jt}, z_{jt} \right\} \in \Psi_j \quad \forall j, \forall t \tag{1d}$$

$$v_{jt}, y_{jt}, z_{jt} \in \{0,1\} \quad \forall j, \forall t \tag{1e}$$

$$\sum_{j \in \Lambda_n^{\mathrm{T}}} p_{jt\omega} + \sum_{i \in \Lambda_n^{\mathrm{W}}} \left(p_{it\omega}^{\mathrm{W}} - p_{it\omega}^{\mathrm{WS}} \right) + \sum_{l \in \Lambda_n^{\mathrm{N}}} p_{lt}^{\mathrm{N}} = D_{nt\omega} - d_{nt\omega}^{\mathrm{LS}} + \sum_{m \in \Lambda_n^{\mathrm{L}}} B_{nm} \left(\theta_{nt\omega} - \theta_{mt\omega} \right) \quad \forall n, \forall t, \forall \omega \tag{1f}$$

$$\underline{P}_j v_{jt} \le p_{jt\omega} \le \overline{P}_j v_{jt} \quad \forall j, \forall t, \forall \omega \tag{1g}$$

$$p_{jt\omega} - p_{j,t-1,\omega} \le R_j^{\mathrm{U}} v_{j,t-1} + S_j^{\mathrm{U}} y_{jt} \quad \forall j, \forall t, \forall \omega \tag{1h}$$

$$p_{j,t-1,\omega} - p_{jt\omega} \le R_j^{\mathrm{D}} v_{jt} + S_j^{\mathrm{D}} z_{jt} \quad \forall j, \forall t, \forall \omega \tag{1i}$$

$$0 \le p_{it\omega}^{\mathrm{WS}} \le p_{it\omega}^{\mathrm{W}} \quad \forall i, \forall t, \forall \omega \tag{1j}$$

$$0 \le d_{nt\omega}^{\mathrm{LS}} \le D_{nt\omega} \quad \forall n, \forall t, \forall \omega \tag{1k}$$

$$B_{nm} \left(\theta_{nt\omega} - \theta_{mt\omega} \right) \le \overline{P}_{nm}^{\mathrm{L}} \quad \forall n, \forall m \in \Lambda_n^{\mathrm{L}}, \forall t, \forall \omega \tag{1l}$$

$$\theta_{nt\omega} = 0 \quad n = n^{\mathrm{Ref}}, \forall t, \forall \omega \tag{1m}$$

$$p_{j,0,\omega} = p_j^{\mathrm{ini}} \quad \forall j, \forall \omega \tag{1n}$$

The objective function (1a) includes: ① first-stage scheduling costs (no-load, start-up, and shut-down); ② second-stage cost (expected production cost); and ③ load-shedding cost.

In the first stage, constraint (1b) enforces the running logic of each thermal generating unit. Constraint (1c) sets the initial status of each thermal unit. Constraint (1d) enforces the minimum up and down time requirements. Constraint (1e) declares that the commitment variables are binary.

In the second stage, constraint (1f) states the power balance per bus, hour, and scenario. Constraints (1g)-(1i) enforce the capacity and ramping limits for thermal generating units per hour and scenario. Constraint (1j) bounds the generation spillages per weather-dependent unit, hour, and scenario. Constraint (1k) limits the load-shedding amounts per demand, hour, and scenario. Constraint (1l) imposes capacity limits on transmission lines per hour and scenario. Constraint (1m) sets the voltage angle of the reference bus to zero per hour and scenario. Constraint (1n) enforces the initial power output of each thermal unit per scenario.

III. Solution Procedure

In this section, we describe the envelope scenarios considered and the quality metric used.

A. Envelope Scenarios

For each time period, we identify two scenarios: the one with the highest net-load and the one with the lowest net-load, and save the corresponding nodal demand and weather-dependent generation data into two new scenarios. This is the way in which the two envelope scenarios are obtained, which is illustrated in Algorithm 1.

Algorithm 1: obtaining envelope scenarios

1: **Input**: demand and weather generation data: $\left(D_{nt\omega}^{\mathrm{A}}, p_{it\omega}^{\mathrm{WA}} \right)$, $\omega \in \Omega^{\mathrm{A}}$

2: Calculate the system net-load $D_{t\omega}^{\mathrm{NL}}$:

$$D_{t\omega}^{\mathrm{NL}} = \sum_n D_{nt\omega}^{\mathrm{A}} - \sum_i p_{it\omega}^{\mathrm{WA}} \quad \forall \omega \in \Omega^{\mathrm{A}}, \forall t$$

3: **for** $t = 1$ to T **do**

4: Find the scenarios representing the maximum and minimum system net-loads:

$$\begin{cases} \overline{\omega} = \arg\max_{\omega} D_{t\omega}^{\mathrm{NL}} \\ \underline{\omega} = \arg\min_{\omega} D_{t\omega}^{\mathrm{NL}} \end{cases}$$

5: Save the demand and weather generation data into two new scenarios corresponding to the upper and lower bounds of the envelope, respectively.

For the upper envelope scenario:

$$\begin{cases} D_{n,t,1}^{\mathrm{E}} = D_{n,t,\overline{\omega}}^{\mathrm{A}} & \forall n \\ p_{i,t,1}^{\mathrm{WE}} = p_{i,t,\overline{\omega}}^{\mathrm{WA}} & \forall i \end{cases}$$

For the lower envelope scenario:

$$\begin{cases} D_{n,t,2}^{\mathrm{E}} = D_{n,t,\underline{\omega}}^{\mathrm{A}} & \forall n \\ p_{i,t,2}^{\mathrm{WE}} = p_{i,t,\underline{\omega}}^{\mathrm{WA}} & \forall i \end{cases}$$

6: **end for**

7: **Output**: demand and weather generation data for the envelope scenarios: $\left(D_{n,t,1}^{\mathrm{E}}, p_{i,t,1}^{\mathrm{WE}} \right)$ and $\left(D_{n,t,2}^{\mathrm{E}}, p_{i,t,2}^{\mathrm{WE}} \right)$

We note that for each time period, the system net-load of the upper/lower envelope scenario is equal to the maximum/minimum net-load among all scenarios in Ω^{A}. Figure 1 provides an illustrative example of the envelop scenarios. The gray lines correspond to the net-load curves for all scenarios in Ω^{A}. The red line with triangle symbols identifies the net-load curve of the upper envelope scenario. The orange line with cross symbols identifies the net-load curve of the lower envelope scenario.

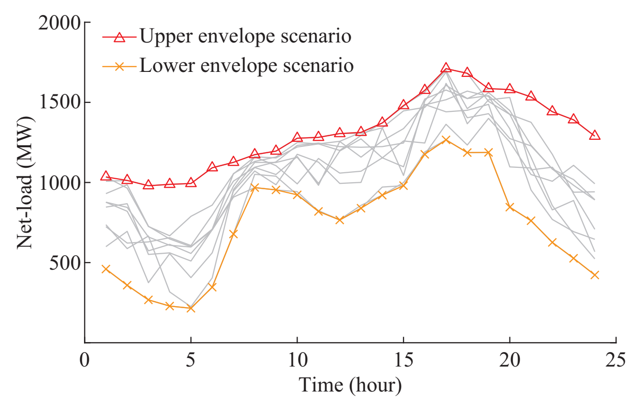

Fig. 1. Envelope scenarios.

B. Solution Quality Metric

For sake of comparison, we consider four problems.

1) Problem A: Problem (1) with the original scenario set Ω^{A}.

2) Problem B: Problem (1) with the average scenario.

3) Problem C: Problem (1) with the upper envelope scenario.

4) Problem D: Problem (1) with the two envelope scenarios.

Problem A is a standard SUC problem, and this is the benchmark problem. Problems B and C are deterministic UC problems. The average scenario used in Problem B is the mean of all scenarios in the original scenario set Ω^{A}. Problem D is a quasi-deterministic UC problem. This problem has the same structure as the SUC problem, while its computational performance is close to that of a deterministic UC problem.

To comprehensively assess the quality of the commitment decisions obtained by Problems B, C, and D, we use both in-sample and out-of-sample analyses, as follows.

1) In-sample Analysis

The solution quality is measured by the similarity of the commitment decisions obtained from Problems B, C, and D with those obtained from Problem A. To mitigate the disturbance caused by the presence of multiple very similar commitment solutions and to compare commitment decisions fairly, we use the following steps for each instance:

Step 1: solve Problem A. Obtain the total cost (c^{A}) and load-shedding amount, as the benchmark.

Step 2: solve Problem B, C, or D, and obtain the commitment decisions.

Step 3: solve Problem A fixing binary commitment decisions as the values obtained in *Step 2*. Obtain the total cost (c^{E}) and the load-shedding amount.

Step 4: calculate the relative cost difference $Gap=\left(c^{E}-c^{A}\right)/c^{A}$.

We assess the quality of the commitment decisions obtained from Problems B, C, and D via the total cost gap and load-shedding difference. Regarding cost gap calculation, we do not include load-shedding cost since it is reported separately. Costs c^{A} and c^{E} include both the scheduling and expected production costs. Note that *Steps 1-3* use the same initial values [25].

2) Out-of-sample Analysis

For the out-of-sample analysis, we select or generate out-of-sample scenarios and, based on them, solve multi-period economic dispatch problems using the commitment decisions obtained from solving Problems A, B, C, and D. Then, we compare the production cost, load-shedding, and ramping violations of each case.

IV. Illustrative Example

In this section, we use a single-node system to illustrate the rationale of the proposed proxy. For the sake of clarity, this example spans two periods.

A. Data

This system is composed of three thermal generating units, a wind unit, and a single demand. For sake of clarity, we neglect transmission constraints in this example. The system diagram is shown in Fig. 2. We use the same technical limits for the three thermal generating units, as shown in Table I. The initial statuses and variable costs for the three thermal generating units are provided in Table II. The start-up, shut-down, and no-load costs for each unit are \$10, \$5, and \$2, respectively. The variable cost for the wind unit is 0.01 \$/MWh. The load-shedding cost is 100 \$/MWh.

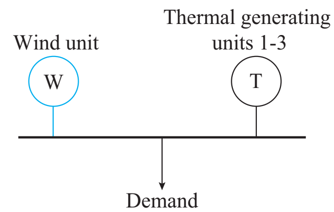

Fig. 2. Diagram of single-node system.

TABLE I
TECHNICAL DATA FOR THERMAL GENERATING UNITS

Parameter	Value
$\underline{P}_j$, $\overline{P}_j$ (MW)	0, 2
S_j^{U}, S_j^{D} (MW)	1, 1
R_j^{U}, R_j^{D} (MW/h)	1, 1

TABLE II
INITIAL STATUSES AND VARIABLE COSTS FOR THERMAL GENERATING UNITS

Unit (j)	v_j^{ini}	p_j^{ini} (MW)	c_j^{V} (\$/MWh)
1	1	1	1.1
2	0	0	1.2
3	0	0	1.3

To illustrate the features of the proposed proxy, we consider two representative cases. In each case, the original scenario set includes two scenarios. Table III provides the demand and wind generation data for each scenario in all cases. In Table III, the third and fourth columns provide system demands during periods 1 and 2. The fifth and sixth columns provide wind generation data.

TABLE III
DEMAND AND WIND GENERATION DATA

Case	Scenario	Demand (MW)		Wind generation (MW)	
		Period 1	Period 2	Period 1	Period 2
I	1	6	5	5	2
	2	4	4	1	3
II	1	5	7	2	4
	2	5	5	5	2

B. Outcomes

Following Algorithm 1, we first compute the system net-load for all scenarios, as shown in Table IV. Note that during period 0, the system net-load is consistent with the initial status of thermal generating units. Then, based on that, we generate envelope scenarios for all cases.

TABLE IV
SYSTEM NET-LOAD

Case	Scenario	System net-load (MW)		
		Period 0	Period 1	Period 2
I	1	1	1	3
	2	1	3	1
II	1	1	3	3
	2	1	0	3

1) *Case I*

In the original scenario set of Case I, scenario 2 has the highest net-load during period 1, while scenario 1 has the highest net-load during period 2. Thus, in the upper envelope scenario, during period 1, we use the demand and wind generation data from scenario 2; while during period 2, we use the data from scenario 1.

Table V provides the demand and wind generation data in Case I. The first row gives the data for the average scenario. The second and third rows provide the data for the first and the second envelope scenarios, respectively. Figure 3 shows net-load curves of the original and generated scenarios in Case I. The gray solid and dashed lines correspond to the net-load curves for the original scenarios. The green line represents the net-load curve of the average scenario. The red and orange lines are the net-load curves for the upper and the lower envelope scenarios, respectively.

TABLE V
DEMAND AND WIND GENERATION DATA IN CASE I

Scenario	Demand (MW)		Wind generation (MW)	
	Period 1	Period 2	Period 1	Period 2
Average	5	4.5	3	2.5
Upper envelope	4	5.0	1	2.0
Lower envelope	6	4.0	5	3.0

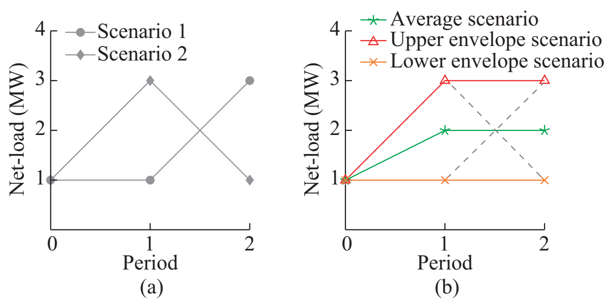

Fig. 3. Net-load curves of scenarios in Case I. (a) Original scenarios. (b) Generated scenarios.

Using the original and generated scenarios, we solve Problems A-D. Table VI provides the solutions obtained by solving each problem. We note that the commitment decisions obtained by solving Problem C (using the upper envelope scenario in Table V) and Problem D (using the upper and lower envelope scenarios) are identical to the ones obtained by solving Problem A. On the contrary, the solution obtained by solving Problem B (using the average scenario) commits less units. Such a solution is not secure since it cannot satisfy the system demand in each of the two original scenarios.

TABLE VI
SOLUTIONS TO COMMITMENT DECISIONS IN CASE I

Unit	Problems A, C, and D		Problem B	
	Period 1	Period 2	Period 1	Period 2
1	1	1	1	1
2	1	1	0	0
3	0	0	0	0

2) *Case II*

Figure 4 provides the net-load curves of the original and generated scenarios in Case II. We note that in the original scenario 2, the system has a significant ramp-up requirement between periods 1 and 2. Such a requirement needs three generating units on line. The lower envelope scenario captures this requirement, while the upper envelope scenario does not.

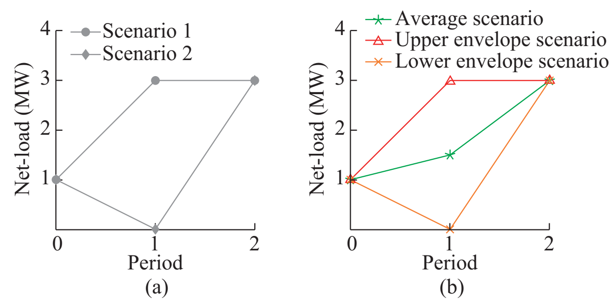

Fig. 4. Net-load curves of scenarios in Case II. (a) Original scenarios. (b) Generated scenarios.

Table VII provides the solutions obtained by solving Problems A-D. We note that commitment decisions obtained by solving Problems A and D are identical, while the ones obtained by solving Problem C commit a lower number of units.

TABLE VII
SOLUTIONS TO COMMITMENT DECISIONS IN CASE II

Unit	Problems A and D		Problem B		Problem C	
	Period 1	Period 2	Period 1	Period 2	Period 1	Period 2
1	1	1	1	1	1	1
2	1	1	0	1	1	1
3	0	1	0	0	0	0

From Cases I and II, we note that the upper envelope scenario captures critical information for the system, the highest net-load requirement. On the other hand, the lower envelope scenario extracts the key information to integrate renewable production, the system ramping requirements.

Solving Problem C results in a secure solution that commits sufficient units to satisfy the system demand. If the renewable generation fluctuates slightly in the original scenario set, like in Case I, the commitment obtained by solving Problem C is identical to that obtained by solving Problem A.

On the contrary, if the renewable generation fluctuates significantly in the original scenario set, like in Case II, the commitment obtained by solving Problem C is different from that obtained by solving Problem A. Such a commitment is secure but lacks system ramping capability, which may lead to renewable generation curtailment and higher operating cost. Under such circumstances, the commitment obtained by solving Problem D is more effective to integrate renewable generation by committing additional units to provide appropriate system ramping capability.

V. Case Study

In this section, we test the performance of the proposed proxy using a modified version of the Illinois 200-bus system [31]. Problems A, B, C, and D are solved using CPLEX [32] under JuMP [33] on a server with an Intel Xeon E5-2680 processor clocking at 2.50 GHz with 60 GB of RAM.

A. Data

1) System Structure

The Illinois 200-bus system is a synthetic power system [31]. In the simulation, we increase the wind generation capacity to enhance system uncertainty. The capacity percentages of thermal, wind, and nuclear generating units are 59.8%, 28.2%, and 12.0%, respectively. The DC network data are obtained from [34].

2) Wind and Demand Scenarios

We obtain the demand data from [31] and historical wind generation data from the System Advisor Model (SAM) [35]. Following the scenario generation method in [25], we generate 20 realistic scenarios spanning a month. The first 10 scenarios constitute a large scenario set Ω^A for the in-sample analysis. The other 10 scenarios compose a testing set for the out-of-sample analysis. Figure 1 shows the net-load curves of scenarios in set Ω^A for one day. Figure 5 presents the wind generation ratio for the same day. The gray lines are wind generation ratios among all scenarios in Ω^A. The red and orange lines represent the wind generation ratios of the upper and lower envelope scenarios, respectively.

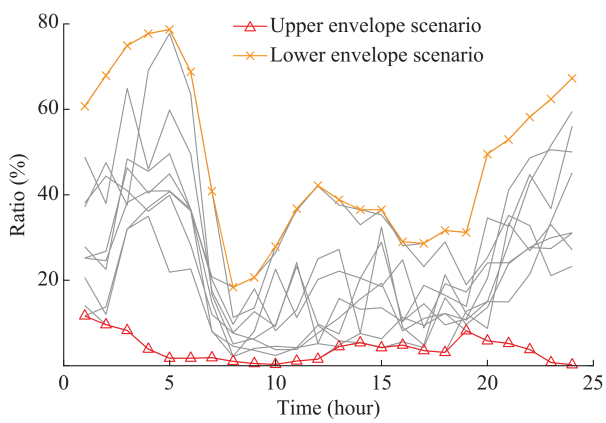

Fig. 5. Wind generation ratio.

B. Simulation Outcomes

We carry out in-sample and out-of-sample analyses over a month (four weeks), which includes 28 instances. To obtain the solution to Problem A in a reasonable time, we set the mixed-integer programming (MIP) solver tolerance as 0.1% and limit the solution time to 2 hours per instance. For a fair comparison, we use the same criteria to solve Problems B, C, and D.

In the benchmark solution, the system exhibits a slight network congestion, as shown in Fig. 6. Figure 6(a) provides the average number of congestion lines among all scenarios for the 28 instances (1 month) on an hourly basis. We note that congestion mainly occurs during peak hours. Figure 6(b) provides the maximum number of congestion lines over all scenarios in a single hour for each day.

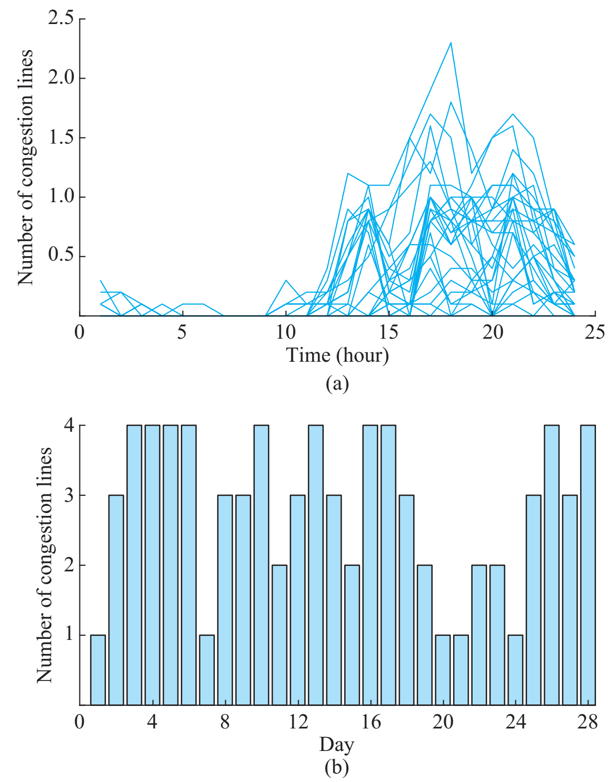

Fig. 6. Network conditions. (a) Number of congestion lines. (b) The maximum number of congestion lines.

1) In-sample Analysis

The solution quality comparison for Problems B, C, and D is provided in Table VIII. The second column lists the number of scenarios included in the corresponding problem. The third column presents the average solution time for each problem in seconds. The fourth column provides the time saving for solving Problems B, C and D as compared to solving the benchmark problem (Problem A). The fifth column presents the average absolute cost gap among all instance. The sixth column provides the maximum absolute cost gap among all instances. The last column provides the ratio of instances whose gap is smaller than 0.01%. Due to this small discrepancy, those solutions can be considered equal. Comparing to the benchmark case, solving Problems B, C and D saves 98%, 94%, and 81% of solution time, respectively. Problem B saves significant solution time, while its solution quality is low. Problem D requires longer solution time than Problem C, while Problem D can obtain a higher number of solutions equal to the benchmark ones.

TABLE VIII
SOLUTION QUALITY COMPARISON

Problem	Number of scenarios	Solution time (s)	Time saved (%)	Average |Gap| (%)	The maximum |Gap| (%)	|Gap| less than 0.01% (%)
A	10	2507				
B	1	44	98	6.25	16.52	0
C	1	159	94	0.02	0.10	64
D	2	476	81	0.01	0.09	75

Figure 7 illustrates the quality of commitment decisions obtained from Problem D for each instance. In Fig. 7(a), the blue line represents the cost gap. For each instance, a positive or negative gap indicates that the commitment decision obtained from Problem D is inferior or superior to the one obtained from Problem A. For reference, we plot the preset CPLEX tolerance of 0.1% as red dashed line. The green and red solid lines are the relative MIP gaps (final gaps) returned from the solver after solving Problems A and D, respectively. The instances with final gaps beyond CPLEX tolerance are stopped due to reaching the 2-hour solving time limit. Figure 7(b) shows the difference in the amount of load-shedding. We note that using the commitment decisions obtained from Problem D results in very small load-shedding difference.

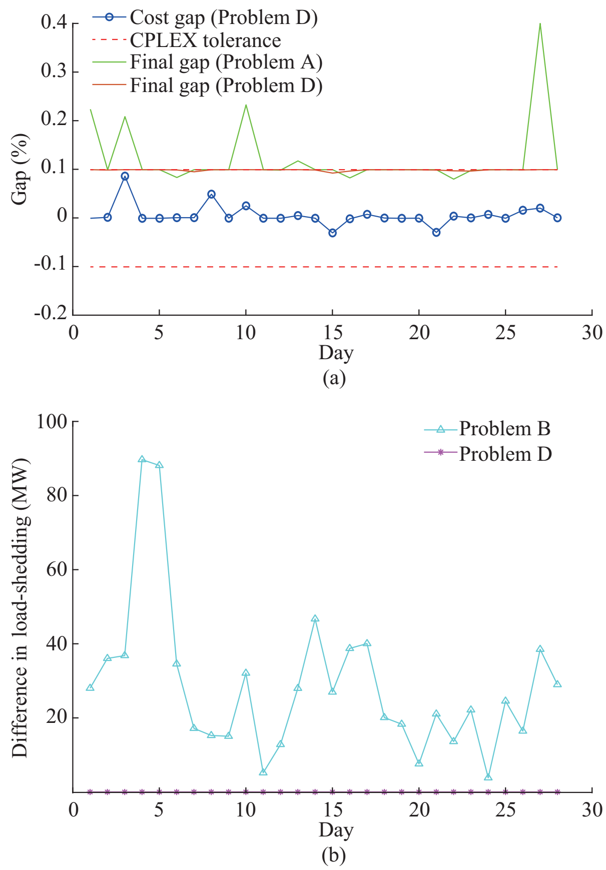

Fig. 7. Solution quality of commitment decisions. (a) Cost gap and final gap. (b) Difference in load-shedding.

Figure 8 provides a comparison of commitment decisions obtained from Problems A and D for days 23 and 24. The red blocks and black crosses represent the online units based on the solution obtained by Problems A and D, respectively. The gray blocks represent wind and nuclear generating units. Problem D is selected here due to its higher accuracy. In Fig. 7(a), we note that the cost gaps for most days are very small. However, the commitment decisions from the two problems are not the same. This is caused by the fact that the problem has multiple solutions that are very similar in cost.

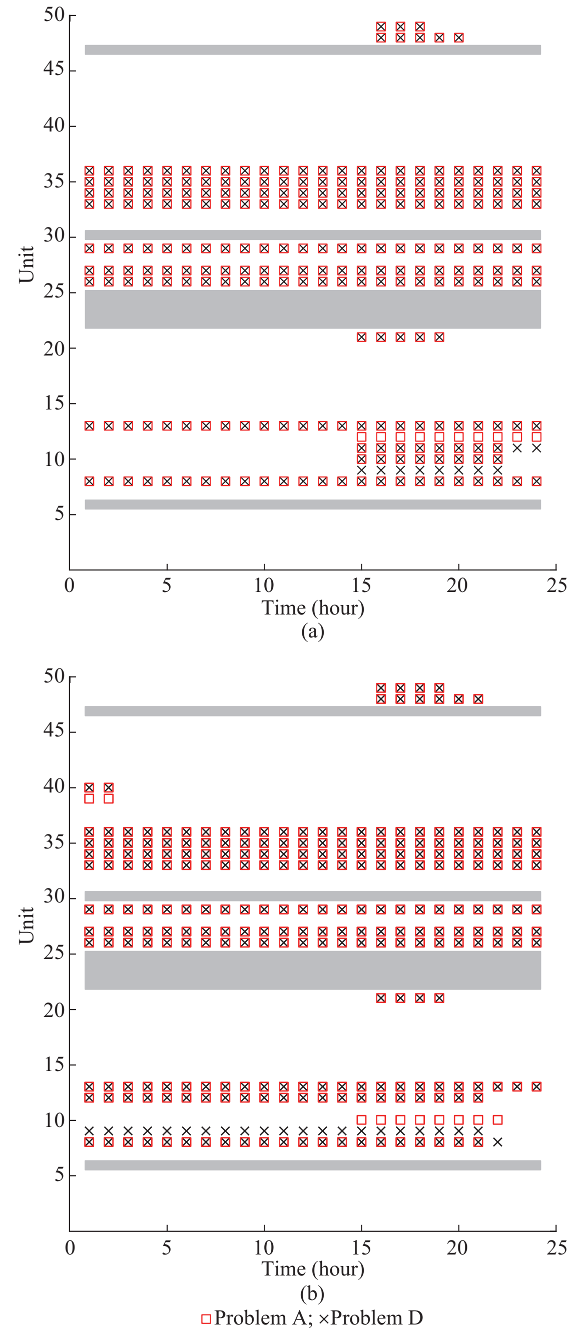

Fig. 8. Commitment decisions. (a) Day 23. (b) Day 24.

2) Out-of-sample Analysis

Using the commitment decision obtained from Problems A, B, C, and D in the previous in-sample analysis, we solve the corresponding multi-period economic dispatch problem [25] with the out-of-sample scenario set for a whole month. Then, we compare the performance of such commitment decisions via total costs (scheduling cost and production cost), load-shedding amount, and ramping violations.

Table IX provides the simulation results. In this table, the first column identifies the problem solved to obtain the commitment decisions. The second column gives the average total cost for all instances over all scenarios. The third column provides the average load-shedding amount over all instances and all scenarios. The last two columns provide ramp-up and ramp-down violations on average.

TABLE IX
SIMULATION RESULTS OF OUT-OF-SAMPLE ANALYSIS

Commitment decision from	Total cost (10^5 $)	Load-shedding (MW)	Ramp-up violation (MW)	Ramp-down violation (MW)
Problem A	5.4067	0.021	0.012	0.015
Problem B	5.0709	1.400	0.559	0.337
Problem C	5.4091	0.020	0.012	0.011
Problem D	5.4065	0.021	0.012	0.016

We note that the total cost is almost the same by using commitment decisions obtained from Problems A and D. Using the commitment decisions obtained from Problem C results in slightly higher cost but lower load-shedding. This is so because the solution of Problem C commits slightly more units to meet the upper envelope scenario. On the other hand, we note that most ramping violations occur at the beginning of the day (hours 1-2) and during the periods before peak hours when the net-load ramps up (hours 15-18). These violations, which are minor, are caused by the initial status of the units prior to hour 1 (hours 1-2), and an insufficient number of available online units before peak hours to meet the system ramping-up needs (hours 15-18). We emphasize that the load-shedding amount and ramping insufficiency are minor and can be easily corrected by the operator.

VI. CONCLUSION

This paper proposes an effective quasi-deterministic proxy for the SUC problem with DC network constraints. By solving the proposed proxy with envelope scenarios, we can obtain commitment decisions almost identical to those obtained by solving the SUC problem, but using significantly less time. From the numerical experiment, the conclusions below are in order.

1) Solving the deterministic UC with just the upper envelope scenario generally results in a relatively conservative unit schedule that satisfies the demand, while having a slightly higher cost than that of the SUC. Such a schedule commits sufficient online generation capacities to satisfy system security requirements. This security information is embedded in the upper envelope scenario that represents an extreme operating condition with very limited renewable generation.

2) Solving the quasi-deterministic proxy with the two envelope scenarios generally results in a very accurate unit schedule that provides sufficient security at the minimum cost. Such a schedule effectively incorporates renewable generation by internalizing system ramping requirements, therefore reducing operating costs. This ramping requirement information is embedded in the lower envelope scenario.

3) The commitment decisions obtained by the proposed proxy do not result in infeasibility issues. From the in-sample and out-of-sample analyses, we conclude that the proposed proxy can quickly produce very similar commitment decisions as those obtained from the SUC problem, and is resilient to network congestion.

Overall, the solution time of the proposed quasi-deterministic proxy is very close to that of a deterministic UC problem. The commitment decisions obtained from the proposed proxy are very similar to the ones obtained from the SUC problem. The proposed quasi-deterministic proxy can be easily implemented in current operation and planning software.

REFERENCES

[1] X. Liu and A. J. Conejo, "Day-ahead reserve determination in power systems with high renewable penetration," *International Journal of Electrical Power & Energy Systems*, vol. 156, p. 109703, Feb. 2024.

[2] A. J. Conejo and L. Baringo, *Power System Operations.* New York: Springer, 2018.

[3] M. F. Anjos and A. J. Conejo, "Unit commitment in electric energy systems," *Foundations and Trends in Electric Energy Systems*, vol. 1, no. 4, pp. 220-310, Dec. 2017.

[4] B. Rachunok, A. Staid, J. P. Watson *et al.*, "Stochastic unit commitment performance considering Monte Carlo wind power scenarios," in *Proceedings of 2018 IEEE International Conference on Probabilistic Methods Applied to Power Systems*, Boise, USA, Jun. 2018, pp. 1-6.

[5] C. Zhao and Y. Guan, "Data-driven stochastic unit commitment for integrating wind generation," *IEEE Transactions on Power Systems*, vol. 31, no. 4, pp. 2587-2596, Jul. 2016.

[6] A. Papavasiliou, S. S. Oren, and B. Rountree, "Applying high performance computing to transmission-constrained stochastic unit commitment for renewable energy integration," *IEEE Transactions on Power Systems*, vol. 30, no. 3, pp. 1109-1120, May 2015.

[7] M. R. Scuzziato, E. C. Finardi, and A. Frangioni, "Comparing spatial and scenario decomposition for stochastic hydrothermal unit commitment problems," *IEEE Transactions on Sustainable Energy*, vol. 9, no. 3, pp. 1307-1317, Jul. 2018.

[8] G. E. Constante-Flores, A. J. Conejo, and R. M. Lima, "Stochastic scheduling of generating units with weekly energy storage: a hybrid decomposition approach," *International Journal of Electrical Power & Energy Systems*, vol. 145, p. 108613, Feb. 2023.

[9] J. Zou, S. Ahmed, and X. A. Sun, "Multistage stochastic unit commitment using stochastic dual dynamic integer programming," *IEEE Transactions on Power Systems*, vol. 34, no. 3, pp. 1814-1823, May 2019.

[10] D. Bertsimas, E. Litvinov, X. A. Sun *et al.*, "Adaptive robust optimization for the security constrained unit commitment problem," *IEEE Transactions on Power Systems*, vol. 28, no. 1, pp. 52-63, Feb. 2013.

[11] I. Blanco and J. M. Morales, "An efficient robust solution to the two-stage stochastic unit commitment problem," *IEEE Transactions on Power Systems*, vol. 32, no. 6, pp. 4477-4488, Nov. 2017.

[12] E. Du, N. Zhang, C. Kang *et al.*, "Scenario map based stochastic unit commitment," *IEEE Transactions on Power Systems*, vol. 33, no. 5, pp. 4694-4705, Sept. 2018.

[13] T. Li, M. Shahidehpour, and Z. Li, "Risk-constrained bidding strategy with stochastic unit commitment," *IEEE Transactions on Power Systems*, vol. 22, no. 1, pp. 449-458, Feb. 2007.

[14] Q. Wang, J. Wang, and Y. Guan, "Stochastic unit commitment with uncertain demand response," *IEEE Transactions on Power Systems*, vol. 28, no. 1, pp. 562-563, Feb. 2013.

[15] Y. Dvorkin, Y. Wang, H. Pandzic *et al.*, "Comparison of scenario reduction techniques for the stochastic unit commitment," in *Proceedings of 2014 IEEE PES General Meeting | Conference & Exposition*, National Harbor, USA, Jul. 2014, pp. 1-5.

[16] K. Bruninx and E. Delarue, "Scenario reduction techniques and solution stability for stochastic unit commitment problems," in *Proceedings of 2016 IEEE International Energy Conference*, Leuven, Belgium, Apr. 2016, pp. 1-7.

[17] P. A. Ruiz, C. R. Philbrick, and P. W. Sauer, "Modeling approaches

for computational cost reduction in stochastic unit commitment formulations," *IEEE Transactions on Power Systems*, vol. 25, no. 1, pp. 588-589, Dec. 2009.

[18] H. Quan, D. Srinivasan, and A. Khosravi, "Incorporating wind power forecast uncertainties into stochastic unit commitment using neural network-based prediction intervals," *IEEE Transactions on Neural Networks and Learning Systems*, vol. 26, no. 9, pp. 2123-2135, Sept. 2015.

[19] K. Bruninx and E. Delarue, "Endogenous probabilistic reserve sizing and allocation in unit commitment models: cost-effective, reliable, and fast," *IEEE Transactions on Power Systems*, vol. 32, no. 4, pp. 2593-2603, Jul. 2017.

[20] M. Paturet, U. Markovic, S. Delikaraoglou *et al*., "Stochastic unit commitment in low-inertia grids," *IEEE Transactions on Power Systems*, vol. 35, no. 5, pp. 3448-3458, Sept. 2020.

[21] Y. Wang, Q. Xia, and C. Kang, "Unit commitment with volatile node injections by using interval optimization," *IEEE Transactions on Power Systems*, vol. 26, no. 3, pp. 1705-1713, Aug. 2011.

[22] Y. Yu, P. B. Luh, E. Litvinov *et al*., "Grid integration of distributed wind generation: hybrid Markovian and interval unit commitment," *IEEE Transactions on Smart Grid*, vol. 6, no. 6, pp. 3061-3072, Nov. 2015.

[23] Y. Dvorkin, H. Pandžić, M. A. Ortega-Vazquez *et al*., "A hybrid stochastic/interval approach to transmission-constrained unit commitment," *IEEE Transactions on Power Systems*, vol. 30, no. 2, pp. 621-631, Mar. 2015.

[24] F. Mohammadi, M. Sahraei-Ardakani, D. N. Trakas *et al*., "Machine learning assisted stochastic unit commitment during hurricanes with predictable line outages," *IEEE Transactions on Power Systems*, vol. 36, no. 6, pp. 5131-5142, Nov. 2021.

[25] X. Liu, A. J. Conejo, and G. E. C. Flores, "Stochastic unit commitment: model reduction via learning," *Current Sustainable/Renewable Energy Reports*, vol. 10, no. 2, pp. 36-44, Jul. 2023.

[26] Á. S. Xavier, F. Qiu, and S. Ahmed, "Learning to solve large-scale security-constrained unit commitment problems," *INFORMS Journal on Computing*, vol. 2021, no. 2, pp. 739-756, Oct. 2021.

[27] Á. Porras, S. Pineda, J. M. Morales *et al*., "Cost-driven screening of network constraints for the unit commitment problem," *IEEE Transactions on Power Systems*, vol. 38, no. 1, pp. 42-51, Mar. 2022.

[28] S. Pineda, J. M. Morales, and A. Jiménez-Cordero, "Data-driven screening of network constraints for unit commitment," *IEEE Transactions on Power Systems*, vol. 35, no. 5, pp. 3695-3705, Sept. 2020.

[29] Z. Ma, H. Zhong, T. Cheng *et al*., "Redundant and nonbinding transmission constraints identification method combining physical and economic insights of unit commitment," *IEEE Transactions on Power Systems*, vol. 36, no. 4, pp. 3487-3495, Jul. 2021.

[30] O. Stover, P. M. Karve, and S. Mahadevan, "Global sensitivity analysis-based dimension reduction for stochastic unit commitment," *IEEE Transactions on Power Systems*, vol. 39, no. 2, pp. 2775-2785, Mar. 2024.

[31] A. B. Birchfield, T. Xu, K. M. Gegner *et al*., "Grid structural characteristics as validation criteria for synthetic networks," *IEEE Transactions on Power Systems*, vol. 32, no. 4, pp. 3258-3265, Jul. 2017.

[32] CPLEX. (2024, Sept.). IBM's linear programming solver. [Online]. Available: http://www.ilog.com/product/cplex

[33] I. Dunning, J. Huchette, and M. Lubin, "JuMP: a modeling language for mathematical optimization," *SIAM Review*, vol. 59, no. 2, pp. 295-320, Jan. 2017.

[34] R. Lima, G.E. Constante-Flores, A. J. Conejo *et al*. (2022, Jul.). Network-constrained stochastic unit commitment data sets: ACTIVSg200 and ACTIVSg2000. [Online]. Available: https://repository.kaust.edu.sa/handle/10754/679948

[35] N. Blair, A.P. Dobos, J. Freeman *et al*., "System advisor model, SAM 2014.1. 14: general description," National Renewable Energy Lab. (NREL), Golden, USA, Tech. Rep., Feb. 2014.

Xuan Liu received the B.Eng. degree from the Department of Electrical Engineering, Tsinghua University, Beijing, China, in 2018, and the M.S. and Ph.D. degrees from the Department of Electrical and Computer Engineering, The Ohio State University, Columbus, USA, in 2019 and 2024, respectively. He is currently an Engineer with State Grid Economic Technology Research Institute, Beijing, China. His research interests include electricity market, power system operation and planning, optimization theory and its application.

Antonio J. Conejo received the M.S. degree from the Massachusetts Institute of Technology, Cambridge, USA, in 1987, and the Ph.D. degree from the Royal Institute of Technology, Stockholm, Sweden, in 1990. He is currently a Professor in the Department of Integrated Systems Engineering and the Department of Electrical and Computer Engineering, The Ohio State University, Columbus, USA. His research interests include control, operation, planning, economics, and regulation of electric energy system, as well as statistics and optimization theory and its application.